Separation Science and Technology
Publication details, including instructions for authors and subscription information:
http://www.informaworld.com/smpp/title~content=t713708471

Peak Capacity in Field-Flow Fractionation

M. Martin[a]; A. Jaulmes[a]
[a] ECOLE POLYTECHNIQUE LABORATORIE DE CHIMIE ANALYTIQUE PHYSIQUE, PALAISEAU, FRANCE

To cite this Article Martin, M. and Jaulmes, A.(1981) 'Peak Capacity in Field-Flow Fractionation', Separation Science and Technology, 16: 6, 691 — 724
To link to this Article: DOI: 10.1080/01496398108058123
URL: http://dx.doi.org/10.1080/01496398108058123

SEPARATION SCIENCE AND TECHNOLOGY, 16(6), pp. 691-724, 1981

Peak Capacity in Field-Flow Fractionation

M. MARTIN and A. JAULMES

ECOLE POLYTECHNIQUE
LABORATORIE DE CHIMIE ANALYTIQUE PHYSIQUE
91128 – PALAISEAU, FRANCE

ABSTRACT

Field-flow fractionation (FFF) peak capacity values have been computed with only two major assumptions: first, the plate height is supposed the sum of only two contributions, axial molecular diffusion and transversal nonequilibrium, and second, the steric effect has been neglected in the equations of retention and peak broadening.

Several reduced parameters have been defined to generalize the equations and limit the number of variable parameters. It appears that among the already implemented FFF subtechniques for which the elution spectrum is an explicit function of the principal dimension, or mass, of the retained sample (which excludes electrical FFF), sedimentation FFF has some peculiar characteristics due to the fact that the field-induced velocity depends on a particular sample, while in thermal and flow FFF it is the same for all samples of a given type under fixed experimental conditions. For example, in sedimentation FFF, the axial diffusion contribution to the plate height persists at a much larger reduced eluant velocity than for the other techniques.

The effect on the peak capacity of the retention volume, the channel length, the eluant velocity as well as the influence of detection limit and analysis time have been studied. Simple relationships between peak capacity and these parameters are established in the high retention and negligible axial diffusion limits which previal in most experimental situations, and deviations from these limits are discussed. It is shown that for all three

techniques mentioned above there is a maximum retention volume beyond which no sample can elute because of the onset of the steric effect. Under typical conditions, this limiting volume is 25-100 times the channel void volume.

INTRODUCTION

The maximum number of components which can be resolved is an important parameter for characterizing the separation power of a fractionation technique. It can serve as a basis for comparing the relative merits of several separation methods, even if they are quite different in their principles. The concept of peak capacity, which is the maximum number of components which can be separated at unit resolution, has been introduced for application to chromatography (1), and then has been extended to other fractionation methods like electrophoresis, centrifugation (2), isoelectric focusing and density-gradient sedimentation (3).

Peak capacity calculations are almost impossible in some of these techniques, due to the complexity of the separation process, so that assumptions have to be made to get an approximate peak capacity value. If all peaks in liquid chromatography are eluted with the same plate number, N (a relatively reasonable approximation) the peak capacity becomes roughly equal to $\sqrt{N}/2$ when the retention volume of the last eluted component is no larger than 10 times the column void volume.

In field-flow fractionation (FFF), a similar approximation gives rise to the same peak capacity values (4) as in chromatography. However while leading to a very simple result, such an assumption (constant plate number for all the peaks), ignores one of the most interesting features of FFF: the significant increase of the plate number with increasing retention. Of course, during a multi-component separation, such an increase is usually moderated by the concomitant decrease of the sample diffusion coefficient. However, it is likely that the peak capacity in FFF will be larger than predicted by the approximation of a constant plate number.

In the following, use is made of another interesting characteristic of FFF, namely its theoretical tractability. Because of simple and well defined channel geometry, peak capacities can be calculated for several system configurations. The peak capacity depends on a large number of parameters, such as channel length and thickness, solvent flow-rate, field type and strength, as well as physicochemical characteristics of the analytes (molecular weight, size, diffusion coefficient). Therefore, in order to give some generality to the calculations, and reduce the number of parameters influencing peak capacity, we define a set of reduced parameters and make use of dimensionless groups of parameters.

BASIC EQUATIONS

To evaluate the peak capacity in FFF, we have used an iterative computer program which, from a given peak, calculates the characteristics (retention volume and standard deviation) of the following peak by a trial-and-error convergent method so that the resolution R_S between the two peaks is equal to 1. Thus, one just has to enter into the program the characteristics of the first peak and the information necessary to compute retention volumes and standard deviations.

Resolution equation

The resolution of a pair of adjacent peaks 1 and 2 is given by :

$$R_S = \frac{V_{R_2} - V_{R_1}}{2(\sigma_{V_1} + \sigma_{V_2})} \qquad (1)$$

or the difference in retention volume (V_R) between the two peaks divided by four times their average standard deviation σ_V, expressed in volume units. The retention volume and standard deviation of a given sample can be expressed as functions of the channel void volume V_o, its retention factor R, which is its migration velocity relative to the solvent average velocity, and its plate

number N:

$$V_R = \frac{V_o}{R} \tag{2}$$

$$\sigma_V = \frac{V_R}{\sqrt{N}} = \frac{V_o}{R\sqrt{N}} \tag{3}$$

or:

$$\frac{V_R}{V_o} = \frac{1}{R} \tag{4}$$

$$\frac{\sigma_V}{V_o} = \frac{1}{R\sqrt{N}} \tag{5}$$

With the help of Eqs. 4 and 5, the resolution R_S can be expressed as a function of the retention factors and plate numbers of peaks 1 and 2:

$$R_S = \frac{\frac{1}{R_2} - \frac{1}{R_1}}{2\left(\frac{1}{R_1\sqrt{N_1}} + \frac{1}{R_2\sqrt{N_2}}\right)} \tag{6}$$

Eqs. 2 to 6 are valid for Gaussian peaks. In reality, the peaks on the fractogram, which represent the variations of concentration of the analyte as a function of time are not rigorously Gaussian, although the peak shape becomes closer to the Gaussian curve as N increases. For this reason, and because in some instances N can be small, we have slightly modified Eqs. 4 to 6 in the computer calculations. These modifications are given in an appendix, which is available from the authors upon request.

Plate number and plate height

The problem of finding V_{R_2} and σ_{V_2} of the second peak is thus replaced by the problem of finding dimensionless parameters R_2 and N_2 such that R_S in Eq. 6 is equal to 1. Both parameters are related to the basic FFF parameter λ which represents the space

constant of the analyte's exponential concentration profile relative to the channel thickness, w. When R becomes smaller than 0.7, λ is very close to the distance of the analyte center of gravity from the accumulation wall relative to w (5). When the solvent velocity profile is parabolic (in the following, the small distortion of the flow profile from the parabolic one due to the temperature dependence of viscosity in thermal FFF is neglected), R is only a function of λ:

$$R = 6\lambda \left[\left(1+e^{-1/\lambda}\right) / \left(1-e^{-1/\lambda}\right) - 2\lambda \right] \qquad (8)$$

This relationship between R and λ has been experimentally verified for a number of systems in the different FFF subtechniques. In the following, we assume it is valid in the range of retentions considered, except when the steric effect occurs (see below). The plate number is related to the plate height H:

$$N = L/H \qquad (9)$$

where L is the channel length. H is the fundamental parameter describing the peak broadening. Under non-gradient conditions, the plate height of a monodisperse sample is given as the sum of two terms reflecting the contributions of the longitudinal molecular diffusion, and non-equilibrium due to the velocity profile in a channel cross-section (6):

$$H = \frac{2D}{Ru} + \chi \frac{w^2 u}{D} \qquad (10)$$

where D is the diffusion coefficient of the sample, u the solvent average velocity and χ a non-equilibrium dimensionless parameter. In this equation, the relaxation contribution to H (6) has not been taken into account since, in any FFF system, it is possible to stop the solvent flow, inject the sample and restore the solvent flow after enough time is spent for the establishment of the compound's exponential concentration profile. The polydispersity contribution to H is not taken into account here, since in peak capacity calculations, one assumes each peak represents a

monodisperse species. Even if this condition is seldom satisfied for real samples, the peak capacity concept will keep all its significance as an index for separation power evaluation and for comparison of different fractionation techniques. In experimental work, there might be other contributions to the plate height arising from multipaths of different velocities inside the channel, dispersion due to the external parts of the system (injector, detector, connection tubings) or concentration effects. In the following, one assumes that all these contributions are negligible and that the band broadening of a monodisperse sample is satisfactorily represented by Eq. 10. The χ coefficient is a function of λ given by the following equation (7):

$$\chi = \frac{2\lambda^2 F}{R(1-e^{-1/\lambda})} \tag{11}$$

in which F is equal to:

$$F = 2A[6-(1/\lambda)-(A/\lambda)-6\lambda+18\lambda e^{-1/\lambda}]+72\lambda^2(28\lambda^2-10\lambda+1)$$
$$-72\lambda^2 e^{-1/\lambda}(28\lambda^2+10\lambda+7) \tag{12}$$

and A to:

$$A = 12\lambda e^{-1/\lambda} \Big/ (e^{-1/\lambda}-1) \tag{13}$$

Reduced parameters

At this point, it is convenient to introduce the following reduced parameters:

$$h = H/w \tag{14}$$

$$\nu = \frac{uw}{D} \tag{15}$$

h is the reduced plate height and ν the reduced velocity. They are defined quite similarly to the corresponding parameters used in chromatography (8): the average distance for cross-sectional diffusion, which is the particle diameter in the case of

chromatography in packed columns, is replaced here by the FFF channel thickness w. By eliminating u, w and D using Eqs. 10, 14 and 15, the plate height takes the following simple form:

$$h = \frac{2}{R\nu} + \chi\nu \qquad (16)$$

Thus, the reduced plate height of samples with the same retention and reduced velocity should be identical, whatever the actual solvent velocity, sample diffusion coefficient, channel thickness, field type and strength.

However, in a given FFF run, the retention factor generally decreases (the retention volume increases) with increasing sample molecular weight and, hence, decreasing diffusion coefficient. Therefore, as seen in Eq. 15, the reduced velocity increases with increasing retention. It would be convenient to express this effect on ν either in terms of the retention factor R, or in terms of the basic parameter λ. These two ways are equivalent since R and λ are explicitly related through Eq. 8. According to the theory of retention in FFF, D is related to λ by (9)

$$D = U\ w\ \lambda \qquad (17)$$

where U is the field-induced velocity, which might be different for each analyte and as a result depends on retention. In order to get the relationship between D and λ, one needs to express the dependence of U on λ.

In thermal FFF, the diffusion coefficient is simply linked to λ through:

$$D = D_T\ (dT/dx)\ w\ \lambda \qquad (18)$$

where dT/dx is the temperature gradient across the thickness of the channel and D_T the thermal diffusion coefficient. For a given polymer type and for a given solvent D_T does not depend on the molecular weight, and is thus independent of retention (10). Therefore, for thermal FFF, one can write:

$$D = c_T\ \lambda \qquad (19)$$

c_T is a constant in a given run. Comparison of Eqs. 17 and 18 shows that in thermal FFF, U is equal to $D_T(dT/dx)$ and is the same for all samples. In flow FFF, the selectivity is based only on differences in diffusion coefficients and D is simply given by (11):

$$D = U\ w\ \lambda = c_F\ \lambda \tag{20}$$

where U is the cross-flow velocity which is constant in a given run. By implication the proportionality coefficient c_F is also constant. In sedimentation FFF, the field induced velocity is not constant but depends on the retention through the analyte diameter. It is given by Stokes sedimentation law:

$$U = \frac{2r^2\Delta\rho G}{9\eta} \tag{21}$$

where r is the particle radius, $\Delta\rho$ the density difference between the sample and the eluant, G the centrifugal acceleration and η the eluant viscosity. The diffusion coefficient is related to the radius of the equivalent sphere by the Stokes-Einstein law:

$$r = \frac{kT}{6\pi\eta D} \tag{22}$$

where k is the Boltzmann constant and T the absolute temperature. Therefore, after combining Eqs. 17, 21 and 22 and rearranging, one obtains:

$$D = \left[\frac{\Delta\rho G w (kT)^2}{162\ \pi^2\ \eta^3}\right]^{1/3} \lambda^{1/3} = c_S\ \lambda^{1/3} \tag{23}$$

For electrical FFF, there is no simple relationship between D and λ since the retention is determined by the net electrical charge of the analyte which in turn depends on the eluant pH and is not easily related to the diffusion coefficient. Therefore, the following calculations of peak capacity will not apply to the case of electrical FFF.

It thus appears that in the three FFF subtechniques (thermal, flow, sedimentation) for which there is a simple connection between

D and λ, this relationship can be summarized as:

$$D = D_o \lambda^{\gamma} \tag{24}$$

with $\gamma = 1$ for thermal and flow FFF and $\gamma = 1/3$ for sedimentation FFF. D_o is the diffusion coefficient of a sample for which $\lambda = 1$, which is a quasi-unretained compound (R = 0.984). Therefore, the reduced velocity ν can be expressed with the help of Eq. 15 as:

$$\nu = \frac{u\,w}{D_o \lambda^{\gamma}} \tag{25}$$

or

$$\nu = \nu_o / \lambda^{\gamma} \tag{26}$$

where ν_o is the reduced velocity corresponding to $\lambda = 1$, which can thus be called the reduced eluant velocity:

$$\nu_o = uw/D_o \tag{27}$$

According to Eq. 17, $D_o = Uw$ for $\lambda = 1$. Using this result in Eq. 27 gives ν_o as the ratio u/U of the axial eluant velocity to the transversal field-induced velocity of an analyte for which $\lambda = 1$. According to Eqs. 16 and 27, the reduced plate height is then written as:

$$h = \frac{2\lambda^{\gamma}}{R\nu_o} + \frac{\chi \nu_o}{\lambda^{\gamma}} \tag{28}$$

h then depends only on ν_o and λ, where ν_o, in that case, is a constant in a given FFF run, and does not depend on a particular sample.

To complete the dimensionless analysis of the peak capacity calculation scheme, it is necessary to relate the plate number in Eq. 9 to the reduced plate height. This leads to the definition of the reduced channel, length, ζ:

$$\zeta = \frac{L}{w} \tag{29}$$

so that N is given by:

$$N = \frac{\zeta}{h} \tag{30}$$

Summary of reduced equations

The equations with reduced (or dimensionless) parameters necessary to calculate the peak capacity are summarized below, in the form corresponding to Gaussian zones:

$$\begin{cases} R_S = 1 = \dfrac{\dfrac{1}{R_2} - \dfrac{1}{R_1}}{2\left(\dfrac{1}{R_1\sqrt{N_1}} + \dfrac{1}{R_2\sqrt{N_2}}\right)} & (6) \\ N = \dfrac{\zeta}{h} & (30) \\ h = \dfrac{2\lambda^{\gamma}}{R\nu_o} + \dfrac{\chi\nu_o}{\lambda^{\gamma}} & (28) \end{cases}$$

R and χ are functions of λ given by Eqs. 8 and 11-13, respectively. The problem of characterization of the second peak is thus reduced to determining the λ value of this peak so that the resolution becomes equal to one. For this determination, one has to specify three parameters: the reduced channel length ζ, the reduced eluant velocity ν_o and the field type through the coefficient γ. One can note that the field strength (temperature gradient in thermal FFF, cross-flow rate in flow FFF, rpm in sedimentation FFF) is not a parameter to be indicated since it is included in the value of ν_o through the diffusion coefficient of the compound eluting at 1.017 V_o ($R = 0.984$, $\lambda = 1$). Thus the peak capacity will not be changed with increased flow rate and field strength if the diffusion coefficients of compounds eluted at 1.017 V_o are proportional to the flow. Consequently, from a peak capacity point of view, doubling the solvent flow rate is equivalent to increasing the temperature drop in thermal FFF and the cross-flow rate in flow FFF by a factor 2 or by a factor 2.8 times rpm in sedimentation FFF.

Furthermore, Eq. 24 predicts an infinite diffusion coefficient for an unretained compound (λ infinite), which is not meaningless, but simply means that every low molecular weight solute is slightly, even if not perceptibly, retained. Therefore, for computer calculations, one has to specify the R (or λ) value of the first eluted peak. In the following, it has been taken as R = 0.996 (λ = 2, V_R/V_o = 1.004).

Numerical values of the variable parameters for typical FFF previous experiments

At this point, it is useful to give some typical values of the ζ and ν_o parameters for some typical actual FFF experiments.

A recent literature survey has shown that thermal FFF can be successfully applied to most polymers with molecular weight larger than 1000 which are soluble in organic solvents. For such polymers the thermal diffusion coefficient D_T, is nearly independent of the molecular weight and equal to about 10^{-7} $cm^2 s^{-1} °K^{-1}$. If one takes as typical a channel which is 50 cm long and 0.1 mm thick, and which is operated with a temperature drop of 60°C between the two plates and in which the solvent flows at such a rate that the no-field elution time is 5 minutes, one obtains ζ = 5000. ν_o in this case is close to 300. However, these are only indicative values, since in high speed thermal FFF, values up to 2500 for ν_o and 8500 for ζ have been reached (12).

Typical flow FFF channels are about 50 cm long and 0.25mm thick, so that the ζ value is 2000. As previously noted, ν_o is here the ratio of the eluant axial velocity, u, to its transversal (cross-flow) velocity, U. Noting that u is the axial flow rate, $\dot{V}$ divided by the cross-section bw, where b is the channel breadth, and that U is the ratio of the cross-flow rate, $\dot{V}_c$, to the corresponding cross-section bL, one can express ν_o in flow FFF as:

$$\nu_o = \frac{\dot{V}}{\dot{V}_c} \frac{L}{w} = \frac{\dot{V}}{\dot{V}_c} \zeta \qquad (31)$$

The ratio $\dot{V}/\dot{V}_c$ can vary within a large domain, due to the wide range of applications of flow FFF. Experiments have been conducted with ν_o values ranging from about 100 for relatively low molecular weight solutes like proteins (13) to over 2000 for submicron-sized silica or polystyrene latex particles (14).

In sedimentation FFF, ν_o depends on a relatively large number of parameters: flow velocity and channel thickness as well as rotation speed of the centrifuge, viscosity of the suspension, density difference between the solute and the solvent, and temperature. Depending on the application type, the actual conditions may vary widely and so will ν_o. Previous experiments have been carried out at ν_o values ranging from 5000 to over 70000 and ζ values in the range 700-3500 (15,16).

RESULTS AND DISCUSSION

As previously noted, the three parameters γ, characterizing the field type, ν_o, the reduced eluant velocity and ζ, the reduced channel length, must be given for peak capacity calculations. However, the peak capacity depends also on the maximum value of the retention volume and increases with this value, as more space is available for peaks. In the following, we will study the influence of each of these parameters.

Peak capacity and maximum retention volume

In FFF solutes of very small size compared to the channel thickness show a minimum retention volume below which no peak appears. This corresponds to the channel void volume. As the size of the solute increases, the retention volume usually increases. As long as this size remains small enough, there is no limit to the maximum possible retention volume resulting from the separation process. A limit may in practice be set by detectability or analysis time considerations. However, as the solute size increases further, a point is reached where the retention behavior,

(described by Eq. 8), is disturbed. This comes from the fact that, due to its finite size, the center of mass of the solute particle cannot approach closely to the wall. In that case, the normal FFF effect and the steric effect combine together and R is given by (17):

$$R = 6\lambda + 6\alpha \tag{32}$$

with:

$$\alpha = r/w \tag{33}$$

This equation is a limiting expression for small values of both λ and α. When r increases, λ decreases and α increases, so that there is a minimum value of R, which corresponds to a maximum retention volume. One can therefore consider that the maximum peak capacity corresponds to this volume, for which Eq. 32 usually holds. To be correct, one should modify the equations for R and χ to take into account the steric effect. The corrections, however, are small for small λ and α (17), so they are not included in the following calculations.

It is interesting to get an estimate of the limiting R value. By differentiating Eq. 32, one obtains the condition for minimum R:

$$\frac{d\lambda}{dr} = -\frac{d\alpha}{dr} \tag{34}$$

From Eqs. 22, 24 and 33, λ is related to α through:

$$\lambda = \left(\frac{kT}{6\pi\eta w D_o}\right)^{1/\gamma} \frac{1}{\alpha^{1/\gamma}} = \beta\alpha^{-1/\gamma} \tag{35}$$

where the proportionality coefficient β is a constant in a given run. By differentiating and combining with Eq. 34, one obtains the relationship between the limiting values of λ and α:

$$\lambda_{lim} = \gamma\alpha_{lim} \tag{36}$$

where γ, as above, is 1 for thermal and flow FFF and 1/3 for

sedimentation FFF. Therefore, from Eq. 32, one has:

$$R_{lim} = 6\ (1+\gamma)\alpha_{lim} = 6\left(1 + \frac{1}{\gamma}\right)\ \lambda_{lim} \tag{37}$$

These limiting variables can be related to α_o, the α value for a sample for which $\lambda = 1$. If one uses Eq. 35 for both α_{lim} and α_o and combines the results with Eq. 36, one obtains:

$$\lambda_{lim} = (\gamma\alpha_o)^{\frac{1}{1+\gamma}} \tag{38}$$

and:

$$\alpha_{lim} = \left(\frac{\alpha_o}{\gamma^\gamma}\right)^{\frac{1}{1+\gamma}}$$

Then R_{lim} becomes:

$$R_{lim} = 6\left(1 + \frac{1}{\gamma}\right)\ \left(\gamma\alpha_o\right)^{\frac{1}{1+\gamma}} \tag{39}$$

which gives for thermal and flow FFF:

$$R_{lim} = 12\sqrt{\alpha_o} \tag{40}$$

and for sedimentation FFF:

$$R_{lim} = 10.53\ \alpha_o^{3/4} \tag{41}$$

At this point, it is useful to give some typical values of α_o and $1/R_{lim}$. Combination of Eqs. 17, 22, 38 and 40 gives:

$$\alpha_o = \frac{kT}{6\pi\eta U w^2} \tag{42}$$

and

$$1/R_{lim} = (V_R/V_o)_{max} = 0.36\ w\sqrt{\frac{\eta U}{kT}} \tag{43}$$

Numerical values for thermal and flow FFF are easily obtained by replacing U by $D_T\Delta T/w$ and $\dot{V}_c/bL$, respectively. In thermal FFF,

with a temperature drop of 60°C and a cold plate temperature of 20°C, an eluant viscosity of 10^{-2} Poise, w = 0.1mm, and $D_T = 10^{-7}$ $cm^2 s^{-1} °C^{-1}$ one obtains a typical value of $\alpha_o = 3.6\times10^{-6}$, which gives $R_{lim} = 0.023$ or $1/R_{lim} = 44$. In flow FFF, at room temperature with an aqueous eluant ($\eta = 10^{-2}$P) and channel dimensions of 500×20×0.25mm, cross-flows ranging from 10 to 100 ml/hr will give α_o values of 1.2×10^{-5}-1.2×10^{-6}, which correspond to R_{lim} = 0.042 - 0.013 or $1/R_{lim}$ = 24-75. For sedimentation FFF, one has on combining Eqs. 22, 23, 33 and 41:

$$\alpha_o = \left(\frac{3kT}{4\pi\Delta\rho G w^4}\right)^{1/3} \tag{44}$$

and

$$1/R_{lim} = (V_R/V_o)_{max} = 0.14\, w \left(\frac{\Delta\rho G}{kT}\right)^{1/4} \tag{45}$$

For $\Delta\rho$ = 0.1g/ml, w = 0.25mm and G = 300g (or, which is nearly equivalent, w = 0.1mm and G = 12000g), one has $\alpha_o = 9.4\times10^{-5}$, which gives $R_{lim} = 0.010$ or $1/R_{lim} = 100$. The interesting point in the above equations is that the maximum retention volume and, therefore, the maximum peak capacity increases with increasing field strength. The maximum size of the solute which can be analyzed before the occurrence of retention reversal due to the steric effect does, however, decrease with increasing field strength.

The variations of the peak capacity, n (see Eq. 50) with retention volume are shown in Figure 1 for four typical cases, for which $\zeta = 2000$. For curves 1 and 2, $\gamma = 1/3$ and the reduced eluant velocities are 50000 and 5000, respectively. Curves 3 and 4 correspond to $\gamma = 1$ and $\nu_o = 1000$ and 100, respectively. In this figure, like in the following, the peak capacity value corresponding to a given value of (V_R/V_o) is the number of peaks which have been completely eluted before a volume V_R of eluant has flowed through the column plus the fraction of the last eluted

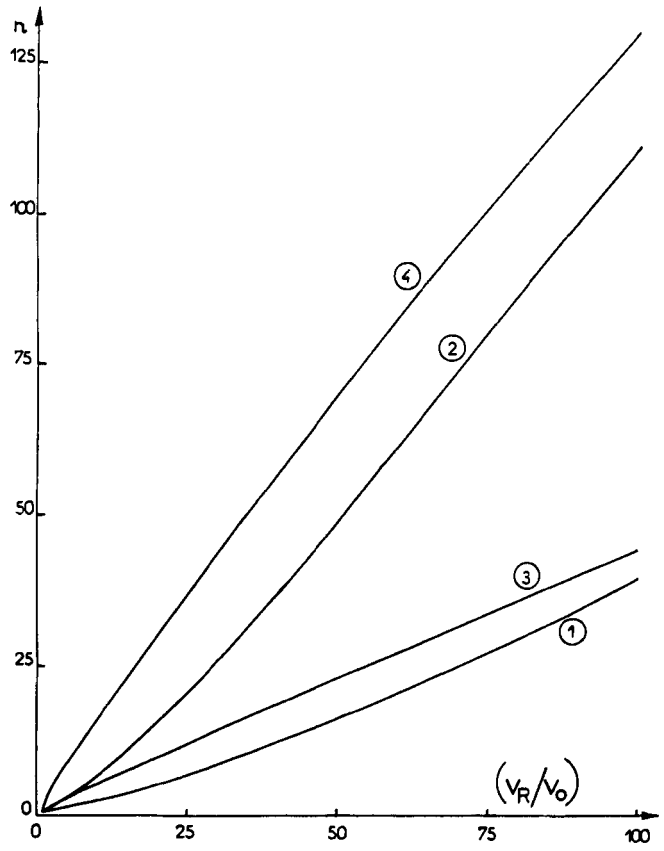

FIGURE 1. Peak capacity versus maximum retention volume at constant channel length and eluant velocity. For all curves: ζ = 2000. Curve 1: γ = 1/3, ν_o = 50000. Curve 2: γ = 1/3, ν_o = 5000. Curve 3: γ = 1, ν_o = 1000. Curve 4: γ = 1, ν_o = 100.

peak which has emerged at V_R. Therefore, all the curves have a common point corresponding to n = 0.5 for V_R/V_o = 1. From Figure 1 it is obvious that the peak capacity increases with V_R/V_o; it is relatively small when V_R/V_o is smaller than 10 (about 3-6 peaks for curves 1, 2 and 3, and 15 peaks for curve 4), but for V_R/V_o larger than 50 it reaches values over 20 in cases 1 and 3, and 50 in cases 2 and 4. Especially noteworthy in Figure 1 is the rate of increase of peak capacity with retention volume. In chromatography

n increases linearly with the logarithm of the retention volume for a constant plate number (1), while in FFF the variation of n with V_R is almost linear for cases where $\gamma = 1$ and still faster for $\gamma = 1/3$. One might explain the difference in behavior between thermal or flow FFF and sedimentation FFF by expressing the rate of generation of peak capacity with retention volume in the limit of high retention. Under these conditions h is mostly determined by the non-equilibrium contribution (this is only an approximation for curves 2 and 4 where, at $V_R/V_o = 100$, axial diffusion accounts for one half and one third of the plate height, respectively). This rate of generation of peak capacity is given by (2)

$$dn = \frac{d(V_R/V_o)}{4\sigma_V/V_o} \tag{46}$$

In the high retention limit, χ is approximated by $1/[9(V_R/V_o)^3]$ and λ by $1/[6(V_R/V_o)]$ within 4% for $(V_R/V_o) > 10$. Then combination of Eqs. 2,3, 28, 30 and 46 gives:

$$dn = \frac{1}{8}\sqrt{6^{2-\gamma}\,\frac{\zeta}{\nu_o}}\;(V_R/V_o)^{\frac{1-\gamma}{2}}\;d(V_R/V_o) \tag{47}$$

After integration, it becomes:

for $\gamma=1$ (thermal and flow FFF)

$$n = 0.31\sqrt{\frac{\zeta}{\nu_o}}\;(V_R/V_o) + \text{const.} \tag{48}$$

and for $\gamma=1/3$ (sedimentation FFF)

$$n = 0.42\sqrt{\frac{\zeta}{\nu_o}}\;(V_R/V_o)^{4/3} + \text{const.} \tag{49}$$

Therefore, in the high retention range when the axial molecular diffusion contribution to peak broadening is negligible, the peak capacity increases linearly with retention volume in thermal and flow FFF and increases as $V_R^{4/3}$ in sedimentation FFF. Since this condition is fulfilled only in the lower part of the high reten-

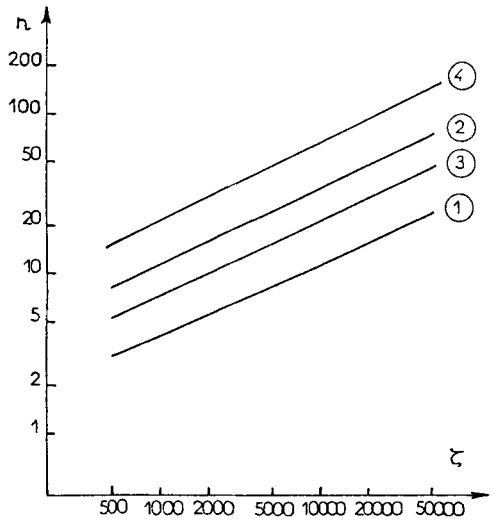

FIGURE 2. Peak capacity versus reduced channel length at constant eluant velocity. $(V_R/V_o)_{max}$ = 20. Same γ and ν_o as for Figure 1.

tion range (V_R/V_o = 10-40) for curve 2, one observes, in that case, a maximum for $dn/d(V_R/V_o)$ around V_R/V_o = 65-70.

Peak capacity and channel length

The variations in peak capacity at V_R/V_o = 20 with reduced channel length are plotted on a logarithmic scale in Figure 2, for the four different cases discussed above. When n is larger than 10-15, these curves are straight lines, all having the same slope equal to 0.5, which means that n increases as the square root of ζ. The slight deviation from this slope at low n values comes from the fact that, according to the above definition of peak capacity, the limiting value is 0.5 when ζ goes to 0. More rigorously, the curve ln(n-0.5) vs ln ζ has a slope of 0.5. The square root dependence of n versus ζ may be understood from Eq. 46 which can be integrated, neglecting the original 0.5 value of n, as:

$$n = \frac{\Delta(V_R/V_o)}{4\,\overline{\sigma_V/V_o}} \qquad (50)$$

where $\Delta(V_R/V_o)$ is the difference in relative retention volume between the last and first peak and $\overline{\sigma_V/V_o}$ the appropriate average relative standard deviation. Comparison with Eq. 1 shows that n represents the resolution between the two extreme peaks of the fractogram multiplied by the ratio of their arithmetical average relative standard deviation to the appropriate average coming from the integration of Eq. 46. According to Eq. 3, $\overline{\sigma_V/V_o}$ can be expressed as $(V_R/V_o)/\sqrt{\overline{N}}$, where (V_R/V_o) relates to either the first or last peak and $\overline{N}$ is the correspondingly appropriate average plate number. As $\overline{N}$ is equal to $\zeta/\overline{h}$, where $\overline{h}$ is the appropriate average plate height, it follows that the peak capacity n, like the resolution between two peaks (18) is proportional to the square root of the reduced channel length.

Peak capacity and eluant velocity

The variations of the peak capacity with the eluant reduced velocity, ν_o, are represented on a logarithmic scale in Figure 3 for thermal and flow FFF (γ=1) and in Figure 4 for sedimentation FFF (γ=1/3). In both figures, ζ has been taken equal to 2000, and four curves have been plotted corresponding to $(V_R/V_o)_{max}$ equal to 10, 20, 50 and 100. The range of velocities is about the same on the logarithmic scale for both figures. However, in Figure 4 the ν_o values are 10 times larger than the values in Figure 3 because of the significant difference in experimental conditions mentioned above. All the curves in these figures show, as a major characteristic, a decrease of n with increasing ν_o. They all are linear with a slope equal to -0.5 for some range of ν_o, which means that for this range, n varies as the reciprocal of the square root of ν_o. This is what is expected from Eqs. 47-49 in the high retention range, in which all the curves are located, when the plate height is only determined by the nonequilibrium contribution (term $\chi\nu$ in equation 16). Deviations from the linearity occur at high velocity

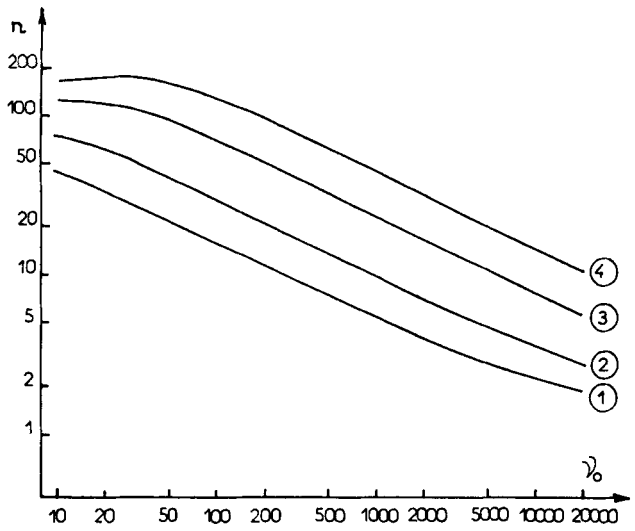

FIGURE 3. Peak capacity versus reduced eluant velocity at constant channel length in thermal and flow FFF (γ = 1). ζ = 2000. $(V_R/V_o)_{max}$ = 10 (curve 1), 20 (curve 2), 50 (curve 3) and 100 curve 4.

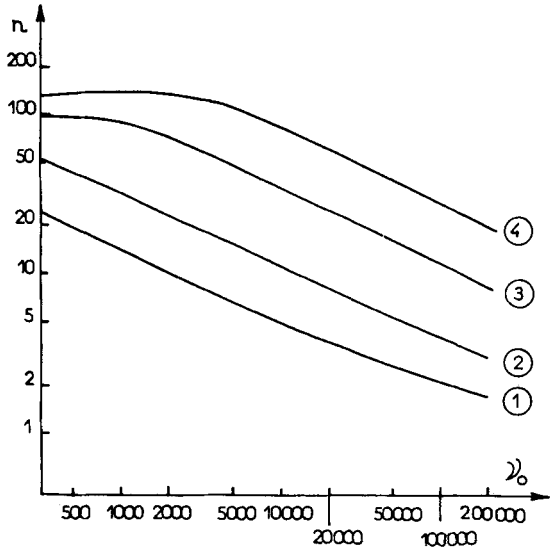

FIGURE 4. Peak capacity versus reduced eluant velocity at constant channel length in sedimentation FFF (γ = 1/3). ζ = 2000. $(V_R/V_o)_{max}$ = 10 (curve 1), 20 (curve 2), 50 (curve 3) and 100 (curve 4).

when n is lower than about 5 because, as noted previously, n has a limiting value of 0.5 when no separation occurs at very high velocity.

Deviations from linearity also appear in the low velocity region, especially for high values of $(V_R/V_o)_{max}$, for which a maximum can be observed. This comes from the fact that nonequilibrium is no longer the only contribution to plate height, and that molecular axial diffusion must be considered. Plate height curves, h vs ν_o, in FFF are characterized by a minimum, the coordinates of which are obtained from Eq. 28

$$h_{min} = 2\sqrt{2\chi/R} \tag{51}$$

$$\nu_{o,opt} = \lambda^{\gamma}\sqrt{2/(R\chi)} \tag{52}$$

Both h_{min} and $\nu_{o,opt}$ depend on λ (or R), but h_{min} does not depend on the field type, while $\nu_{o,opt}$ does through γ. At the optimal velocity, the molecular axial diffusion and the nonequilibrium contribute equally to the plate height. Figure 5 represents the variations of h_{min} with R. The curve has a maximum at $h_{min} = 0.428$, a rather small value, for R = 0.69. As previously noted (19), the minimal plate height decreases with increasing retention and the limiting value of h_{min} for small R is:

$$h_{min} = \frac{2}{3}\sqrt{2}\,R = 0.94\,R \tag{53}$$

Figure 6 represents the variations of $\nu_{o,opt}$ with R for the two values of γ. In contrast to the previous figure, Figure 6 shows that $\nu_{o,opt}$ has a minimal value, which is equal to 2.2 around R = 0.6 for γ=1 and to 7.4 around R = 0.7-0.75 for γ=1/3. In the low retention range, when R goes to 1, $\nu_{o,opt}$ varies as $14.5\,\lambda^{\gamma}$ and thus increases to infinity faster for thermal and flow FFF than for sedimentation FFF. This increase to infinity is due to the fact that according to Eq. 24, D increases to infinity when R goes to 1. This is not important since, in practical situations, one is not able to measure retention factors corresponding to λ values larger than 2 (R = 0.996) or even 1 (R = 0.984). Far more

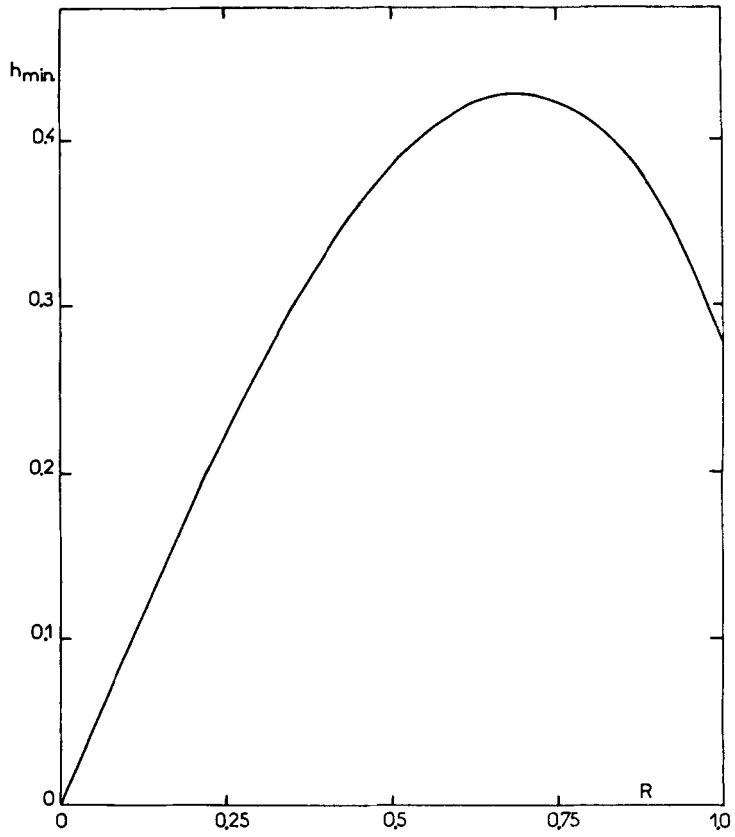

FIGURE 5. Minimum value of the reduced plate height versus retention factor.

significant are the variations of $\nu_{o,opt}$ in the high retention domain. In that range, $\nu_{o,opt}$ can be expressed as:

$$\nu_{o,opt} = \frac{\sqrt{18}}{6^{\gamma}} \frac{1}{R^{(2-\gamma)}} \tag{54}$$

which gives:

for $\gamma = 1$:

$$\nu_{o,opt} = 0.71/R \tag{55}$$

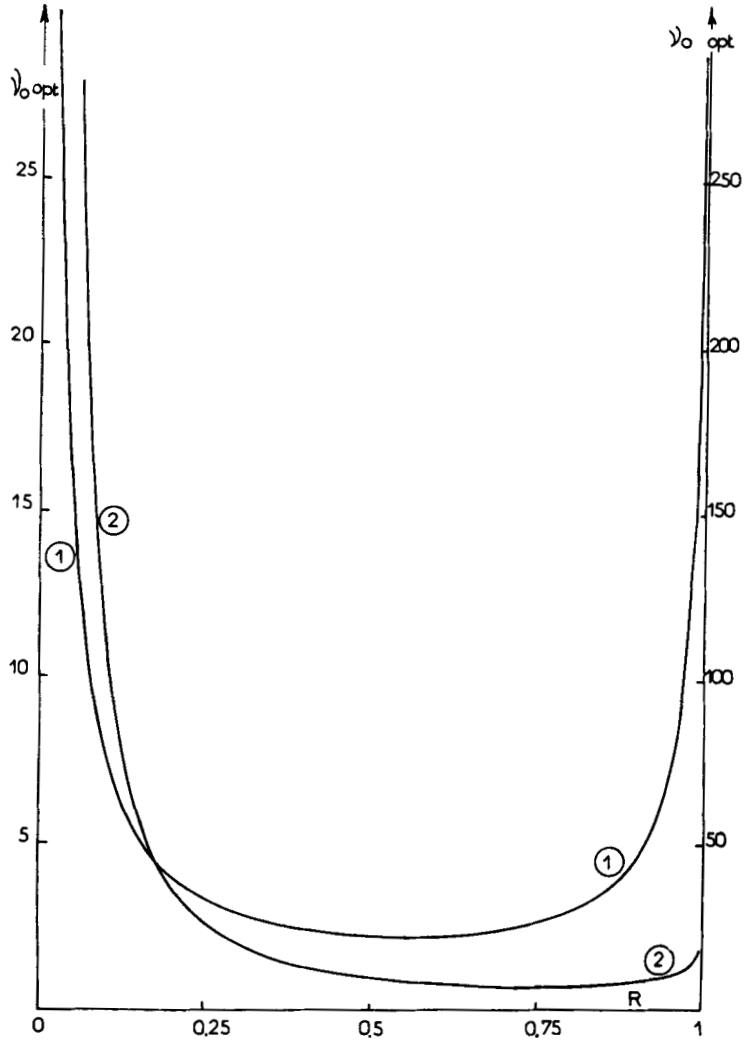

FIGURE 6. Reduced eluant velocity corresponding to the minimum plate height versus retention factor. Curve 1 and left y-axis: $\gamma = 1$ (thermal and flow FFF). Curve 2 and right y-axis: $\gamma = 1/3$ (sedimentation FFF).

and for $\gamma = 1/3$:

$$\nu_{o,opt} = 2.83/R^{5/3} \tag{56}$$

According to these equations, $\nu_{o,opt}$ increases to infinity when R decreases to 0. Therefore, during an FFF run at a constant reduced eluant velocity ν_o, as analytes become more and more retained, axial molecular diffusion accounts for a successively more important relative contribution to plate height. Consequently, the plate height is larger than its nonequilibrium contribution alone. This explains the deviation in the curves in Figures 3 and 4 from the linearity expected on the basis of Eqs. 48 and 49 for the lowest values of ν_o and the highest values of $(V_R/V_o)_{max}$. Since $\nu_{o,opt}$ increases faster with decreasing R in sedimentation FFF than in thermal or flow FFF, this deviation occurs in the first case at higher velocities than in the second. Ultimately, at the lowest values of ν_o and R, axial diffusion becomes the predominant mechanism for band broadening. In that case Eq. 47 must be replaced by:

$$dn = \frac{1}{4}\sqrt{\frac{6\gamma\zeta\nu_o}{2}}\,(V_R/V_o)^{\frac{\gamma-3}{2}}\,d(V_R/V_o) \tag{57}$$

This shows that n in this range increases as the square root of ν_o. Therefore, one will observe for each curve a maximum of n for some value of ν_o, this value being higher in sedimentation FFF than in thermal or flow FFF.

Peak capacity and detectability

The peak capacity may, sometimes, be limited by detectability considerations. Most of the detectors used in FFF, as in liquid chromatography, are concentration sensitive. To be detectable, an analyte must have a concentration C_{max} larger than a minimal detectable concentration at the outlet of the channel. C_{max} can be expressed for a Gaussian zone in terms of the elution parameters previously defined, and the mass m of analyte injected in the channel:

$$C_{max} = \frac{m}{\sigma_V \sqrt{2\pi}} = \frac{m\sqrt{N}}{V_R \sqrt{2\pi}} \tag{58}$$

In liquid chromatography, when the plate number is the same for all the solutes, C_{max}/m decreases with increasing V_R, which may impose a limit of $(V_R/V_o)_{max}$ and consequently on the peak capacity.

Figure 7 represents the variations of the relative standard deviation, σ_V/V_o, of peaks eluting at different retention volumes during the fractionation run for four typical cases corresponding to the same values of ν_o and γ as for the curves in Figure 1, ζ being the same for all curves and equal to 2000. The shapes of the sedimentation FFF curves 1 and 2, on one hand, and of the thermal or flow FFF curves 3 and 4, on the other hand, are markedly different. This difference may be understood if one looks at the high retention limit expression of σ_V/V_o when the first term of the left-hand side of Eq. 28 is negligible:

$$\sigma_V/V_o = 2\sqrt{\frac{\nu_o}{6^{(2-\gamma)}\zeta}} \, (V_R/V_o)^{\frac{\gamma-1}{2}} \tag{59}$$

which gives for $\gamma=1$:

$$\sigma_V/V_o = 0.82\sqrt{\frac{\nu_o}{\zeta}} \tag{60}$$

and for $\gamma = 1/3$:

$$\sigma_V/V_o = 0.45\sqrt{\frac{\nu_o}{\zeta}} \, (V_R/V_o)^{-1/3} \tag{61}$$

In thermal and flow FFF, the standard deviation appears to be independent of retention volume. This is manifested by the quasi-constancy of the curves 1 and 2 for $V_R/V_o > 10$. By contrast, in sedimentation FFF, Eq. 61 indicates that σ_V decreases with increasing V_R as seen in Figure 7 for curves 1 and 2 at $V_R/V_o > 5$. Eqs. 59-61 are valid only in the high retention range; they cannot explain the differences in the shapes of the curves for $V_R/V_o < 10$. All curves show a fast increase of σ_V/V_o with V_R/V_o for V_R close to V_o, as a result of the dependence of $[\chi/(R^2\lambda^\gamma)]^{1/2}$ with (V_R/V_o),

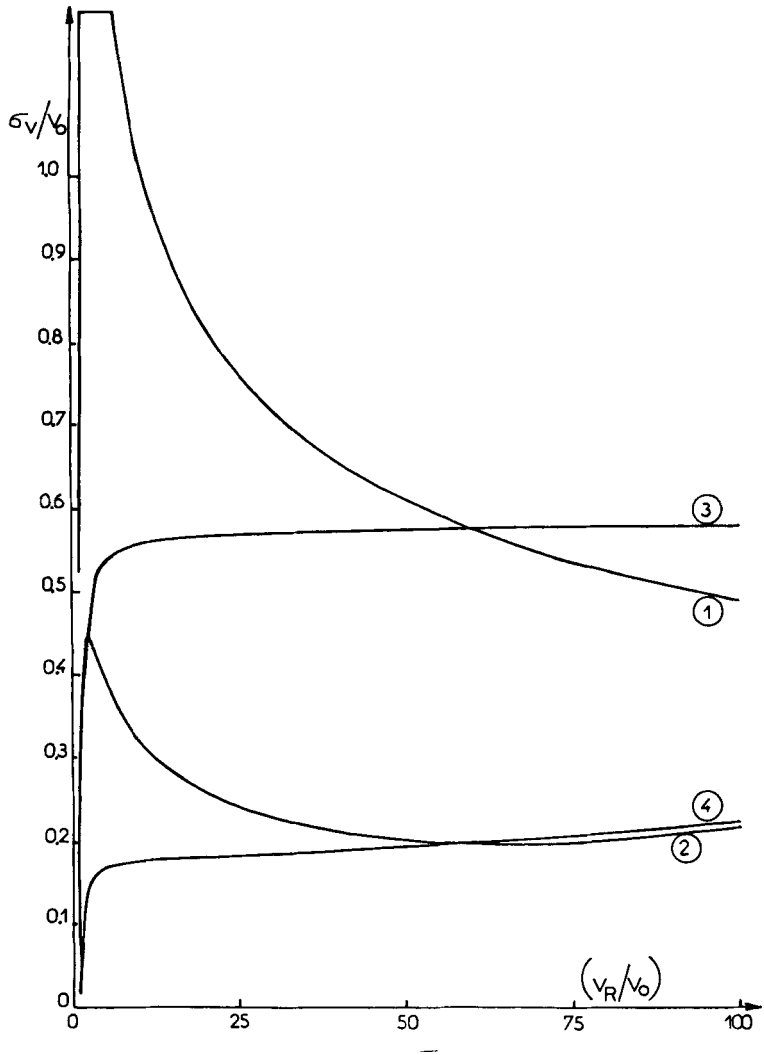

FIGURE 7. Relative peak standard deviation versus relative retention volume. ζ = 2000. Same γ and ν_o as for Figure 1.

since in that retention range axial diffusion is negligible. Therefore, sedimentation FFF curves, which are increasing with V_R at low V_R and decreasing at large V_R, have a maximum around V_R/V_o = 2-3 while thermal and flow FFF curves increase steadily to their constant limit at large V_R. When nonequilibrium is the main band broadening mechanism, σ_V/V_o is proportional to the square root of the eluant reduced velocity, as indicated for the limit of high retention by Eqs. 59-61. Accordingly, the σ_V/V_o values of curves 1 and 3 are about three times higher than the corresponding values of curves 2 and 4. As previously noted, during a given run, where the ratio $\nu_o/\nu_{o,opt}$ decreases with increasing retention volume, the axial diffusion contribution to h may not remain negligible at high V_R. Therefore, deviations from the limits set by Eqs. 60 and 61 are observed for the low ν_o curves 2 and 4 at values of V_R/V_o larger than about 30. They are manifested by an inflection point in curve 4 and a minimum in curve 2.

Since for given values of m and V_o, C_{max} is inversely proportional to (σ_V/V_o), one can easily deduce the variations of C_{max} with V_R/V_o from Figure 7. Therefore, after a sharp decrease from $V_R = V_o$ to $V_R \simeq 2\ V_o$, which is not of interest since resolution is poor in this range, the concentration at the peak maximum for a monodisperse solute either increases, or remains approximately constant with increasing retention volume. This is an interesting characteristic peculiar to FFF. Consequently, under the typical experimental conditions evoked here, the peak capacity will not be limited by detectability considerations.

Peak capacity and analysis time

As seen above, peak capacity is increased by extending the retention volume range for separation. But this increase is achieved at the expense of time. Therefore the peak capacity may be limited by the amount of time allowed for the fractionation. One can try to optimize the peak capacity for a given analysis time. The analysis time is expressed as:

$$t_A = \frac{L}{R_{lim} u} \tag{62}$$

or, by combination with Eqs. 27 and 29:

$$t_A = \frac{w^2}{D_o} \frac{\zeta}{R_{lim} \nu_o} \tag{63}$$

In this equation, the term w^2/D_o is twice the average time required by the solute eluted at R = 0.984 (λ=1) to move a distance w by diffusion. Since, as noted previously, D_o is equal to Uw where U is the field-induced velocity, identical for all solutes in thermal and flow FFF, and corresponding to the solute for which λ=1 in sedimentation FFF. This time w^2/D_o represents also w/U, the time required to move distance w at the field-induced velocity U. Optimization of n at constant t_A can be made in different ways, because there are many variables involved in the expression of t_A.

First of all, one may leave R_{lim} constant and equal to the minimum value of R at which compounds can elute because of the onset of the steric effect. If one assumes w and D_o constant, one is looking at n for a constant ratio ζ/ν_o, which means constant void volume elution time. The optimization problem is then the following: is it better to work with a long channel at a high flow-rate or with a short channel at a low eluant velocity? Figure 8 represents on a logarithmic scale the variations of n with ν_o at constant value of ζ/ν_o for R_{lim} = 1/50 and for four cases. Curves 1 and 2 correspond to sedimentation FFF with the ζ/ν_o ratio equal to 1 and 0.1, respectively, curves 3 and 4 to thermal and flow FFF with ζ/ν_o equal to 1 and 10, respectively. From this figure it appears that the peak capacity is constant in sedimentation FFF for $\nu_o > 5000$ and in thermal and flow FFF practically over all the velocity range. Again the high retention limit with the hypothesis of negligible axial diffusion contribution to plate height, as reflected in Eqs. 48 and 49, allows one to explain this constancy of n. Indeed, according to these equations, n is proportional to the square root of the ζ/ν_o ratio. Therefore, as this ratio is maintained constant, n is constant whatever the actual

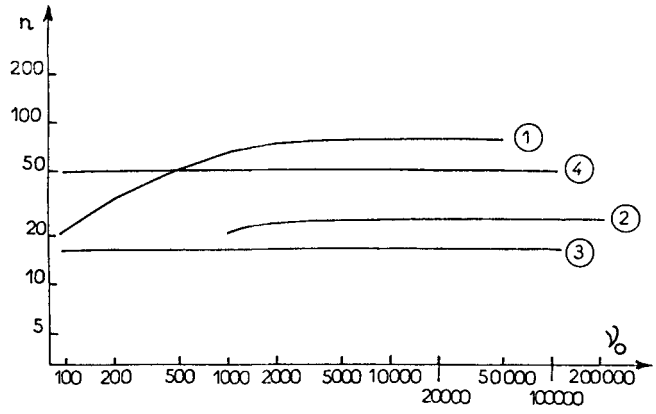

FIGURE 8. Peak capacity versus reduced eluant velocity at constant analysis time. $(V_R/V_o)_{max} = 50$. Curve 1: $\gamma = 1/3$, $\zeta/\nu_o = 1$. Curve 2: $\gamma = 1/3$, $\zeta/\nu_o = 0.1$. Curve 3: $\gamma = 1$, $\zeta/\nu_o = 1$. Curve 4: $\gamma = 1$, $\zeta/\nu_o = 10$.

values of ζ and ν_o. The deviation from this limit for the sedimentation FFF curves at low ν_o is accounted for by the increasing relative contribution of axial diffusion to the plate height with decreasing velocities. When this contribution is predominant, Eq. 57 predicts that n is proportional to $\sqrt{\zeta\nu_o}$ or $\nu_o\sqrt{\zeta/\nu_o}$. Therefore, at low velocity, n varies linearly with ν_o, and the log n versus log ν_o curve should have a slope equal to 1. The shape of curve 1 for ν_o ranging from 100 to 5000 represents the transition between the two limiting forms of n. In summary, from Figure 8, it appears that in order to get the highest peak capacity at constant analysis time, constant field and retention volume range, it does not matter what are the actual values of ν_o and ζ, provided that ν_o is large enough for the axial diffusion contribution to plate height to be negligible. This is in sharp contrast with the optimization result in liquid chromatography where the highest peak capacity is obtained for infinitely large velocity, so that n is, in practice, limited by pressure considerations.

When working with a given FFF channel at a fixed force-field, one may impose a low eluant velocity and stop the analysis after a small volume of liquid has flowed through the column, or one may have the eluant flowing at a high rate and stop the field after a larger retention volume so that the analysis time is the same in the two cases. This is equivalent to maintaining the product $R_{lim}\ \nu_o$ or the ratio $(V_R/V_o)_{max}/\nu_o$ constant in Eq. 63. In the high $\nu_o/\nu_{o,opt}$ range and high retention limit, in which most experimental work is done, Eq. 48 indicates that n is proportional to $(V_R/V_o)_{max}/\sqrt{\nu_o}$ or $\sqrt{\nu_o}\,[(V_R/V_o)_{max}/\nu_o]$. Similarly, Eq. 49 shows that, in sedimentation FFF, n is proportional to $(V_R/V_o)_{max}^{4/3}/\sqrt{\nu_o}$ or $\nu_o^{5/6}[(V_R/V_o)_{max}/\nu_o]^{4/3}$. In both cases, at constant $(V_R/V_o)_{max}/\nu_o$, n is seen to increase with increasing ν_o. This trend is confirmed by the n values reported for different reduced eluant velocities in Table 1 for $\gamma=1/3$ and Table 2 for $\gamma=1$. Therefore the maximum peak capacity at constant analysis time, channel geometry and field, will be obtained at the maximum retention volume compatible with the onset of the steric effect and the associated highest velocity.

TABLE 1

Peak Capacity Values at Constant Analysis Time and Constant $(V_R/V_o)_{max}/\nu_o$ Ratio in Sedimentation FFF

ν_o	$(V_R/V_o)_{max}$	n
10 000	10	4.9
20 000	20	8.1
50 000	50	16.2
100 000	100	28.2

$\gamma=1/3$

$\zeta=2000$

$(V_R/V_o)_{max}/\nu_o=0.001$

TABLE 2

Peak Capacity Values at Constant Analysis Time and Constant $(V_R/V_o)_{max}/\nu_o$ Ratio in Thermal and Flow FFF

ν_o	$(V_R/V_o)_{max}$	n
100	10	15.7
200	20	21.2
500	50	32.1
1000	100	44.6

$\gamma=1$

$\zeta=2000$

$(V_R/V_o)_{max}/\nu_o=0.1$

CONCLUSION

Under present experimental conditions, the peak capacity in FFF reaches about 5 to 100, depending on the actual system used. The present study can serve to easily evaluate the change in peak capacity brought about by a modification of any operational parameter, since all these parameters are grouped in only three reduced variables: the reduced channel length, the reduced eluant velocity and the maximum relative retention volume. The validity of the results depends on the validity of the basic expressions for retention and peak broadening described by Eqs. 8 and 10. Deviations from these equations have sometimes been observed, especially for high retention. While the origin of these deviations is not completely elucidated, one believes that, in most of the cases, they rely directly or indirectly on technological problems and that they will be reduced and, hopefully, eliminated by future progress. For instance, improved detectability will allow a decrease in peak broadening and retention shift associated with injection and concentration nonidealities in the channel. In that light, peak capacity calculations performed in this study give ultimate values based on present experimental conditions.

REFERENCES

1. J.C. Giddings, Anal. Chem. 39, 1027 (1967).
2. J.C. Giddings, Sep. Sci. 4, 181 (1969).
3. J.C. Giddings and K. Dahlgren, Sep. Sci. 6, 345 (1971).
4. J.C. Giddings, Y.H. Yoon and M.N. Myers, Anal. Chem. 47, 126 (1975).
5. M. Martin, M.N. Myers and J.C. Giddings, J. Liq. Chromatog. 2, 147 (1979).
6. L.K. Smith, M.N. Myers and J.C. Giddings, Anal. Chem. 49, 1750 (1977).
7. M. Martin and J.C. Giddings, J. Phys. Chem., to be published.
8. J.C. Giddings, Anal. Chem. 35, 1338 (1963).
9. J.C. Giddings, S.R. Fisher and M.N. Myers, Am. Laboratory 10, 15 (1978).
10. M. Martin and R. Reynaud, Anal. Chem., in press.
11. J. C. Giddings, F.J. Yang and M.N. Myers, Anal. Chem. 48, 1226 (1976).
12. J.C. Giddings, M. Martin and M.N. Myers, J. Chromatog. 158, 419 (1978).
13. J.C. Giddings, F.J.F. Yang and M.N. Myers, Science 193, 1244 (1976).
14. J.C. Giddings, G.C. Lin and M.N. Myers, J. Colloid Interf. Sci. 65, 67 (1978).
15. F.J. Yang, M.N. Myers and J.C. Giddings, J. Colloid Interf. Sci. 60, 574 (1977).
16. K.D. Caldwell, T.T. Nguyen, J.C. Giddings and H.M. Mazzone, J. Virol. Methods 1, 241 (1980).
17. J.C. Giddings, Sep. Sci. Technol. 13, 241 (1978).
18. J.C. Giddings,"Dynamics of Chromatography, Part I." Principles and Theory, Dekker, New York, 1965.
19. J.C. Giddings, Sep. Sci. 8, 567 (1973).

LIST OF SYMBOLS

b	channel breadth
c	cross-section average concentration
c_F	proportionality constant in Eq. 20 for flow FFF
c_S	proportionality constant in Eq. 23 for sedimentation FFF
c_T	proportionality constant in Eq. 19 for thermal FFF
h	reduced plate height
k	Boltzmann constant
m	mass of analyte injected in the channel
n	peak capacity
r	spherically equivalent analyte radius
t	time
t_A	analysis time
t_R	retention time
u	eluant average velocity
w	channel thickness
z	coordinate along the channel length
A	factor in the expression of F (Eq. 11)
C_{max}	concentration at the maximum of the peak at the outlet of the channel
$\mathcal{D}$	effective dispersion coefficient
D	diffusion coefficient
D_o	diffusion coefficient corresponding to $\lambda=1$
D_T	thermal diffusion coefficient
F	factor in the expression of χ (Eq. 11)
G	centrifugal acceleration
H	plate height
J	molar flux density
L	channel length
N	plate number
N_{app}	apparent plate number
R	retention factor
R_S	resolution
T	temperature
U	velocity induced by the field on the analyte

V_o channel void volume

V_R retention volume

$\dot{V}$ axial flow-rate

$\dot{V}_c$ cross-flow rate in flow FFF

α ratio of the spherical equivalent analyte radius to the channel thickness

α_o α value corresponding to $\lambda=1$

β proportionality constant in Eq. 35

γ exponent in Eq. 23

ζ reduced channel length

ν eluant viscosity

λ basic FFF parameter = space constant of the analyte exponential concentration profile relative to the channel thickness

ν reduced velocity

ν_o reduced eluant velocity

$\Delta\rho$ density difference between analyte and eluant

σ_t peak standard deviation in time unit

σ_V peak standard deviation in volume unit

σ_z peak standard deviation in distance unit

τ reduced time

χ nonequilibrium dimensionless parameter